ARTICLE

Structures and Properties of Supported Polyimide/SnO_2 Hybrid Membranes

Mao-gong Wang, Shun-he Zhong*

College of Chemical Engineering and Technology, Tianjin University, Tianjin 300072, China

(Dated: Received on July 5, 2006; Accepted on October 10, 2006)

A series of polyimide/SnO_2 hybrid membranes supported on TiO_2/kieselguhr-mullite were prepared from polyimide with a large amount of carboxyl and SnO_2 sol via a sol-gel process. The SnO_2 phase chemically linked with the polyimide through the pendant carboxyl along the polyimide. The hybrid membranes were highly homogeneous, and when the SnO_2 contents reached 15wt% the SnO_2 phase was observed as particles with a diameter of 5 nm dispersed in the hybrid membranes . The cross-linking between the SnO_2 phase and polyimide effectively enhanced the glass temperature of the hybrid films. With the increasing of the SnO_2 contents, the pore sizes of the membranes decreased, and their pore sizes were mainly focused on 3.8, 3.1, 2.8 and 2.4 nm. The hybrid membranes showed higher permeability for H_2, CO_2, CO and H_2O when compared to the pure polyimide. The separation factors of the polyimide/SnO_2 hybrid membranes with 15wt% SnO_2 content for H_2/N_2, CO_2/N_2, CO/N_2 and H_2O/N_2 were 54.1, 30.2, 35.9 and 40.1, respectively.

Key words: Polyimide/SnO_2, Hybrid materials, Imidization, Sol-gel

I. INTRODUCTION

Organic-inorganic hybrid materials have been recognized as an important class of new-generation materials which combine the desirable properties of the ceramic phase and organic polymers and exhibit outstanding properties in terms of thermal stability, mechanical properties, gas permeability and permeselectivity [1-3]. In recent years, hybrid materials have been extensively studied and utilized in many fields such as microelectronics, optoelectronic devices, adhesion, sensors and membranes [4-7]. Among the various approaches used to prepare hybrid materials, the sol-gel route provides a unique and versatile method. The final morphology and properties of the hybrid material can be controlled by the optimization of several synthetic parameters, such as the type of the solvent, the ratio of water and catalyst to the alkoxide, the reaction temperature and pressure, and the concentration of the reactants [8,9].

During the past few years, polyimide membranes containing inorganic oxide have been widely studied. Our previous studies showed that different types of inorganic oxide in the hybrid membranes could influence the properties of the hybrid membranes, especially the gas separation property [10-12]. Up to now, such data on the polyimide/SnO_2 membranes have not been reported. Tin dioxide (SnO_2) is one of the most widely used semiconductor oxides due to its chemical and mechanical stabilities. It can be used as transparent electrodes for solar cells and liquid crystal displays; catalysts for methanol conversion and CO/O_2, CO/NO reaction in the control of noxious emissions; antistatic coatings; gas sensors; anodes for lithiumion batteries; transistors; catalyst supports; nano and ultrafiltration membranes; and anticorrosion coatings [13-17]. Therefore, the study of the polyimide/SnO_2 hybrid materials is important for its new application in the field of membrane separation.

In the reported literature, the morphology and physical properties of the hybrid materials and effects of synthetic variables of the sol-gel process have been investigated for a number of polymeric systems. For example, Nandi *et al.* prepared polyimide/SiO_2 hybrid via the "site isolation method" [18]. This method consisted of pre-binding an alkoxide precursor to a polyamic acid, forming a carboxylate group and subsequently curing the system to imidize the polyamic acid and to drive the sol-gel reaction. The hybrid material had fine compatibility of the organic and inorganic phases. However, the hybrid had some disadvantages, such as brittleness and incomplete imidization. Yen and co-workers prepared polyimide/SiO_2 hybrid material through intrachain coupling by 3-aminopropyl trimethoxysilane (APrTEOS) and interchain hydrogen bonding by g-glycidyloxypropyltrimethoxysilanes (GOTMS). The hybrid was homogenous and thermally stable. The glass transition temperature of the hybrid was hardly enhanced because interchain hydrogen bonding is feeble. In this study, in order to enhance the linking of the organic and inorganic phases, we prepared polyimide/SnO_2 hybrid membranes through introducing additional functionalities along the polyimide backbone by adding 3,5-diaminobenzoic acid (DABA). These functional groups can chemically connect with the SnO_2 phase. The morphologies, chemical structures, thermal performances, pore distribution and gas permeability properties of the hybrid membranes were characterized and elucidated.

*Author to whom correspondence should be addressed. E-mail: shzhong@tju.edu.cn

TABLE I Quantity and ratios of the reactants in the preparation of hybrid sol (1.0000 g Polyimide)

Samples	$Sn(OC_2H_5)_4{\cdot}2C_2H_5OH$/g	$[H_2O]/[Sn^{4+}]$	$[H^+]^a/[Sn^{4+}]$	SnO_2wt%[b]
PIS00	–	–	–	–
PIS03	0.0802	2	0.1	3
PIS07	0.1951	2	0.1	7
PIS15	0.4575	2	0.1	15

[a] The HCl used is a 37% HCl solution.
[b] The stannum content indicates the wt% SnO_2 in the composite.

II. EXPERIMENTS

A. Materials

The 4,4'-hexafluoroisopropylidenediphthalic anhydride (6FDA), 2,4,6-trimethyl-1,3-phenylen-ediamine (TMPDA) and 3,5-diaminobenzoic acid (DABA) were obtained from Fluka Chemical Co. (Buchs, Switzerland). Prior to use, the reagents 6FDA and TMPDA were purified by sublimation and DABA was recrystallized in methanol. The N,N-Dimethylacetamide (DMAc) was obtained from Sinopharm Chemical Reagent Co., Ltd. (Shanghai, China). The DMAc was dehydrated prior to use by 0.3 nm molecular sieves for 24 h followed by vacuum distillation. The Tin(IV) alkoxide ($Sn(OC_2H_5)_4{\cdot}2C_2H_5OH$) was synthesized according to the previously reported methods [19].

B. Polyimide preparation

The polyimide preparation was based on 6FDA (8 mmol, 3.554 g), TMPDA (4 mmol, 0.601 g) and DABA (4 mmol, 0.609 g). A total solvent of DMAc (25 mL) was used to dissolve these three reagents respectively, and give a 20wt% polymer solution. The TMPDA and DABA solution were first added to a previously dried 150 mL three-necked round bottom flask with vigorous stirring and N_2 purged at 25 °C. Then the 6FDA solution was slowly added into the flask. Finally, the homogenous and viscous polyamic acid (PAA) was formed after constantly stirring the reactants for 24 h at 25 °C in a N_2 purged atmosphere. Chemical imidization of the above prepared PAA was carried out by adding a mixture of acetic anhydride (0.04 mol, 4.084 g), triethylamine (0.04 mol, 4.048 g), and 30 mL DMAc into the PAA solution with vigorous stirring for 30 min at 25 °C, and then in a 60 °C silicon oil bath for another 24 h. The homogeneous solution was subsequently poured into ethanol absolute, precipitated, filtered out and dried in a vacuum oven at 160 °C for 24 h to obtain the 6FDA-TMPDA-DABA polyimide.

C. SnO_2 sol preparation

The SnO_2 sol was generated using a 1:30:2:0.1 molar ratio of $Sn(OC_2H_5)_4{\cdot}2C_2H_5OH$, DMAc, H_2O and HCl. Firstly, 11.721 g of $Sn(OC_2H_5)_4{\cdot}2C_2H_5OH$ was dissolved into 83.4 mL DMAc forming the transparent solution. Secondly, 0.25 mL HCl (37wt%) dissolved in 0.89 mL deionzed water was added dropwise to the solution with vigorous stirring. Finally, the above mixed solution was stirred for 2 h and the homogeneous transparent SnO_2 sol was obtained. In this reaction, the stoichiometric amount of water was added taking into account the quantity present in the acid catalyst solution.

D. Hybrid sol preparation

The preparation of the hybrid sol was based on the reaction of the homogeneous organic and inorganic solution. Firstly, 1.0 g of the above prepared 6FDA-TMPDA-DABA polyimide was dissolved into 10.6 mL DMAc to form a 10% polyimide solution. Secondly, a certain amount of SnO_2 sol was added into the polyimide solution and stirred for other 12 h. Finally, a viscous and homogeneous polyimide/SnO_2 solution was formed. In this study, a series of hybrid sols with different SnO_2 contents was prepared. Table I summarizes the amounts of reactants used in the preparation of the hybrid sol.

E. Supported membrane preparation

The membrane supports were the kieselguhr-mullite (K-M) tubes with a smooth TiO_2 intermediate layer membrane. The K-M supports are of an average pore size 2.01 μm, porosity of 0.42 μm^3 by volume and compressive strength above 4.5 MPa [20]. The TiO_2 membrane is of good micromorphology and uniform pore size distribution of pore size around 37 nm [21]. The whole process of supported membrane preparation included cleaning, impregnating, drying and calcining. At first, the TiO_2/K-M membrane tubes were cleared by deionized water in a CQ-50 ultrasonic regenerator for 30 min, then vacuum dried at 120 °C for 3 h. Then these clean and dry membrane tubes were dipped into the hybrid sol for 5 min, and air dried in a clean environment for 48 h. This extended time interval was chosen to minimize solvent concentration gradients on the membrane surface during evaporation. Finally, they were cured by

ISSN 1003-7713/DOI:10.1360/cjcp2007.20(2).197.6

steps in vacuum conditions employing heating intervals of 60 °C for 5 h, 120 °C for 5 h and then 220 °C for 12 h.

F. Methods characterization

The thermal stability of the polyimide/SnO_2 hybrid materials was investigated using the Perkin-Elmer Pyris 6 TGA and Diamond DSC instruments. The FTIR spectra were recorded by a Thermo Nicolet NEXUS FTIR spectrometer. A transmission electron microscope, a Tecnai G2 F20, was employed in evaluating the hybrids' morphology. X-ray photoelectron spectroscopy (XPS) measurement of hybrids was performed using an ESCA PHI1600 spectrometer equipped with a Mg Kα X-ray source. The pore distribution of the membranes was determined with a Quantachrom Chembet 3000 by N_2 adsorption measurement.

The gas separation property of the membranes was measured as function of mean pressure by using the following gases: H_2, CO_2, CO, N_2, and H_2O. The pressure drop across the membrane could be adjusted by adjusting the downstream valve and measured by pressure gauges. The pressure of the membrane outside was kept at 101 kPa, and the mean pressure was 5.33 kPa. Among the gases, H_2, CO_2, CO and N_2 were measured at room temperature, and H_2O was measured at 120 °C. The membrane tube was mounted into a stainless steel membrane separator and sealed by silicone rubber and graphite gaskets. The area of the membrane was 6.5×10^{-3} m^2.

III. RESULTS AND DISCUSSION

A. FT-IR

Figure 1 shows the FTIR spectra of the PIS00, PIS03, PIS07 and PIS15. In the spectra, the characteristic imide groups are observed at the following peaks: 1780 cm^{-1} (C=O asym. str.), 1720 cm^{-1} (C=O sym. str.) and 1370 cm^{-1} (C−N str.). The C−NH stretching band was not observed at 1660 cm^{-1} [22], which indicates the successful chemical imidization of the pure polyimide. In the FTIR spectra, the bands in the region from 780 cm^{-1} to 400 cm^{-1} increase with increasing SnO_2 contents, due to the presence of a broad band associated with the vibration of the Sn−O bond [15]. The band at 1125-1035 cm^{-1} is assigned to the Sn−O−C bending mode [23], which is formed by the reaction between the pendant carboxyl and the SnO_2 sol phase.

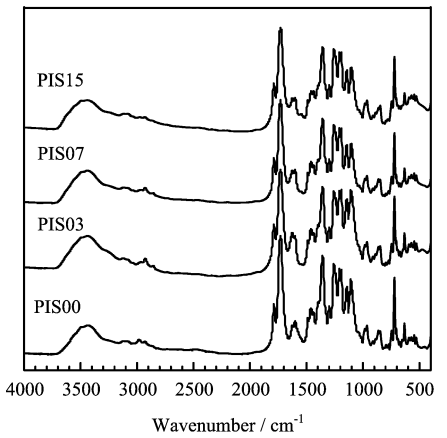

FIG. 1 FTIR spectra of the membrane materials.

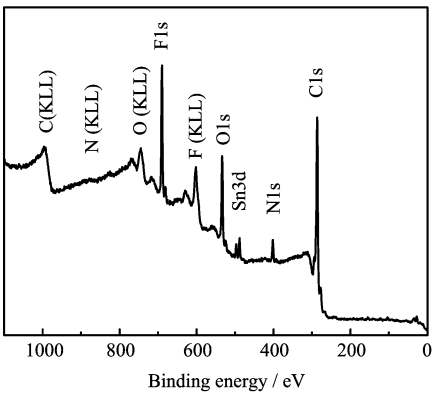

FIG. 2 XPS survey spectrum of the PIS07 hybrid membrane.

B. XPS

Figure 2 shows the XPS low-resolution (survey) spectrum of the PIS07 hybrid membrane. The spectrum indicates the presence of carbon, nitrogen, oxygen, fluorine and tin. Figure 3 shows the XPS high-resolution (multiplex) spectra of the C1s, O1s, F1s, N1s and Sn3d in the PIS07 hybrid membrane. The C1s line consists of three components: the most intense peak at 284.7 eV, a well-defined shoulder at 287.9 eV and weaker peak at 292.7 eV. The first peak is attributed to the carbon atoms of the benzene rings and the methyl. The shoulder peak is attributed to the carbon atoms of the carbonyl. The weaker peak is attributed to the carbon atoms of the $-CF_3$ of the 6FDA structure. The F1s, O1s and N1s lines contain a single peak, and their banding energies were 688.2, 531.7 and 399.9 eV, respectively. The above atoms and bonds are the main part of the 6FDA-TMPDA-DABA polyimide structure. The Sn3d line contains two peaks at 495.2 and 486.7 eV for $Sn3d^3$ and $Sn3d^5$ respectively, which indicate that the Tin atom exists in the hybrid membrane as Tin dioxide. Based on the results of the FTIR and XPS, the chemical structure of the polyimide/SnO_2 is shown in Fig.4.

C. Thermal stability of the hybrid materials

The thermal decomposition temperature (T_d), glass transition temperature (T_g) and the residue of the mem-

ISSN 1003-7713/DOI:10.1360/cjcp2007.20(2).197.6

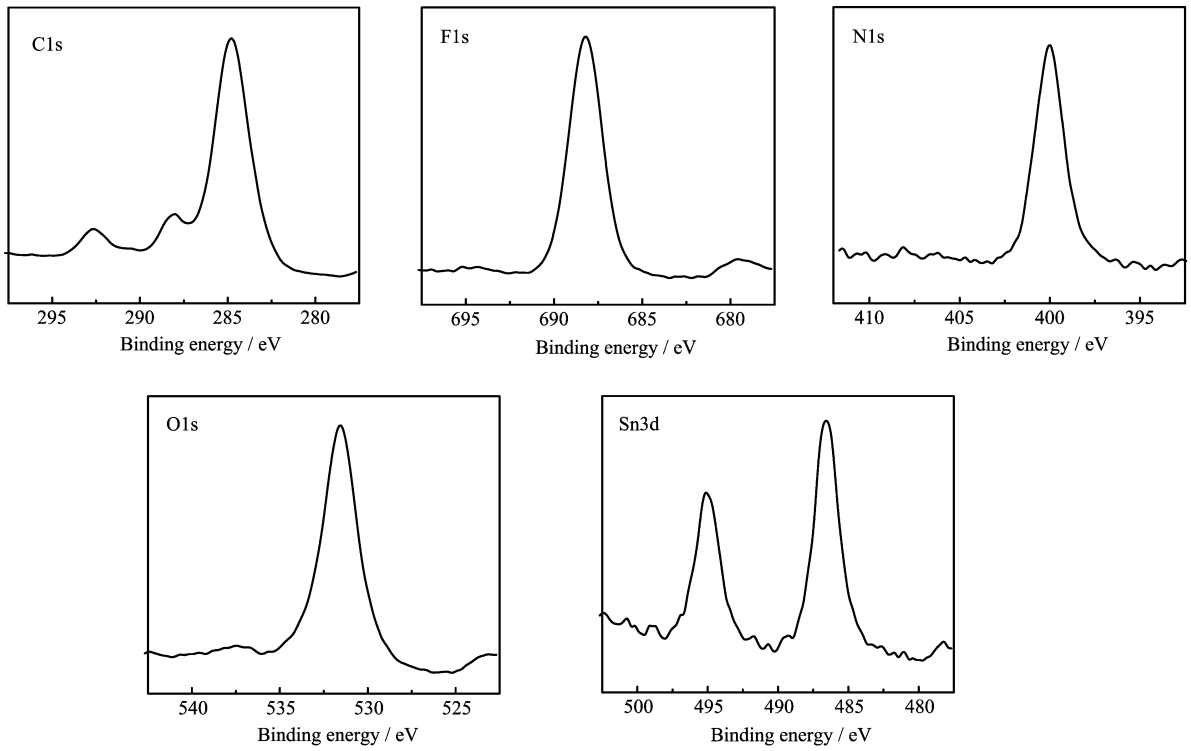

FIG. 3 XPS spectra of C1s, O1s, F1s, N1s and Sn3d in the PIS07 hybrid membrane.

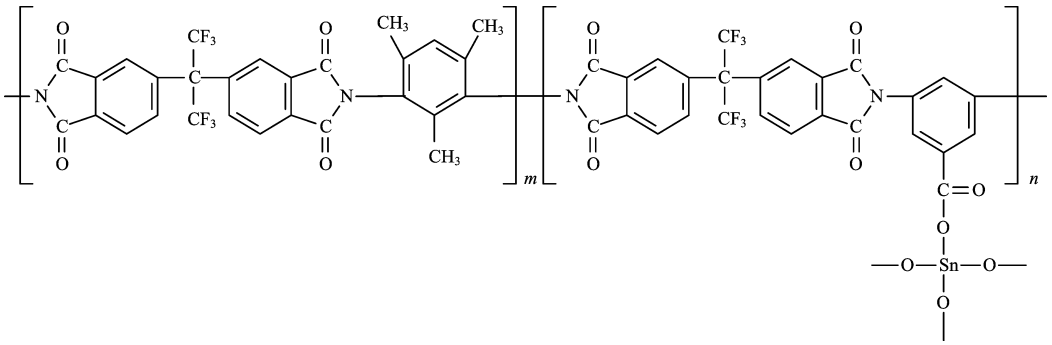

FIG. 4 The structure model of the polyimide/SnO_2 hybrid materials.

branes at 800 °C are shown in Table II. Figure 5 shows the TGA curves of the PIS00, PIS03, PIS07 and PIS15. As shown in the results determined by the DSC, the T_g of the PIS00, PIS03, PIS07 and PIS15 increases with the increase of the SnO_2 contents. Corresponding to the results of the FTIR, the polyimide chain was covalently bonded to the SnO_2 phase via the pendant carboxyl, which restricted the mobility of the polyimide chain and thus enhanced the T_g. The T_d of the PIS00, PIS03, PIS07 and PIS15 decreased with the increasing SnO_2 content. This is probably attributable to the metal-catalyzed oxidation decomposition effect of the trace mount of free SnO_2 in the hybrid membranes. This phenomenon also happened in the studies of Chiang on BAO-ODPA polyimide/TiO_2 hybrid mateial [24]. The final residues are the SnO_2 and carbon residue after the polyimide decomposition.

D. Microstructure of the samples

Figure 6 shows the TEM images of the PIS07 and PIS15 hybrid membranes. The morphology of the PIS07 is quite homogeneous and appears to have a very fine dispersion of SnO_2 phase. When the SnO_2 content reached 15wt%, the SnO_2 domains were observed with sizes about 5 nm, which is smaller than the reported sizes at the same metal oxide contents [25-27]. The introduction of the pendant carboxyl along the main polyimide chain provides the benefit in prohibiting the separation of the SnO_2 phase and improving the com-

ISSN 1003-7713/DOI:10.1360/cjcp2007.20(2).197.6

TABLE II The thermal properties of the PIS00, PIS03, PIS07 and PIS15

Samples	T_d[a]/°C	T_g[b]/°C	Residue/%
PIS00	520	386	50
PIS03	516	417	54
PIS07	509	425	58
PIS15	491	436	62

[a] T_d, temperature corresponding to 5% weight loss.
[b] T_g, temperature as large groups in the main chain start their segmental motion.

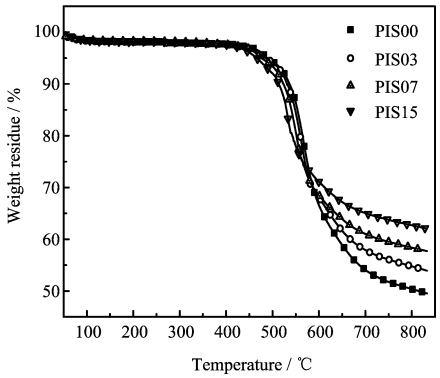

FIG. 5 Thermogravimetric profiles of the PIS00-15 hybrid materials.

patibility of the hybrid.

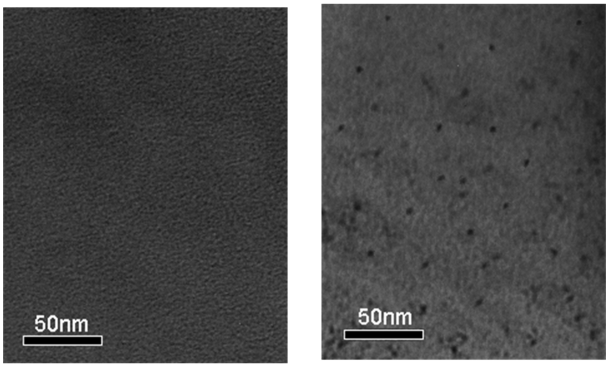

FIG. 6 TEM images of the PIS07 (left) and PIS15 (right) hybrid membranes.

E. Pore distribution of the membranes

Figure 7 shows the pore distribution of the polyimide and polyimide/SnO_2 hybrid membranes. The pore sizes of the PIS00, PIS03, PIS07 and PIS15 membranes are mainly focused on 3.8, 3.1, 2.8 and 2.4 nm respectively. With the increase of the SnO_2 content, the pore sizes of the hybrid membranes decreased. The reason for this is that the SnO_2 phase filled in the polyimide matrix through linking with the pendant carboxyl along the polyimide.

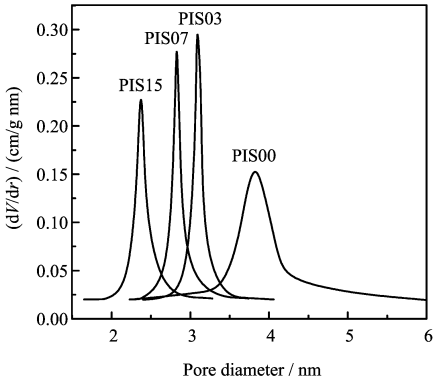

FIG. 7 Pore distribution of the PIS00-15 membranes.

F. Gas permeability of the membranes

The experimental results obtained for various gases are summarized in Table III. With the increase of the SnO_2 content, the permeability of the membranes for the gases decreased and the selectivity increased. Compared with other gases, the permeability of the hybrid membranes for H_2 and CO decreased less and the selectivity increased more with the increase of the SnO_2 content. The hybrid membranes showed finely separation properties for H_2 and CO. Combined with the results of the membranes' pore distribution, we can reason that the SnO_2 phase in the hybrid membranes has adsorption effects on the H_2 and CO, which improved the permeability property of the hybrid membranes for the two gases.

IV. CONCLUSION

A series of polyimide/SnO_2 hybrid membranes were successfully prepared through partially hydrolyzed Tin alkoxide sol chemical bonding with the pendant carboxyl along the polyimide via the condensation reaction. The hybrid membranes were homogeneous and thermally stable. The cross-linking between the SnO_2 phase and polyimide effectively enhanced the glass temperature of the hybrid membranes. The SnO_2 phase was well dispersed in the polyimide matrix, and the SnO_2 phase observed as particles of 5 nm diameter dispersed in the hybrid membranes when the SnO_2 contents reached to 15wt%. With the increase of the SnO_2 content, the pore sizes of the membranes decreased, and the four samples' pore sizes were mainly focused on 3.8, 3.1, 2.8 and 2.4 nm, respectively. The hybrid membranes showed higher separation property for the selected gases compared to the pure polyimide. When the SnO_2 content was 15wt%, the separation factors of

ISSN 1003-7713/DOI:10.1360/cjcp2007.20(2).197.6

TABLE III Gas permeability of the pure polyimide and hybrid membranes

System	Permeability[a]					Separation factors			
	N_2	H_2	CO_2	CO	H_2O	H_2/N_2	CO_2/N_2	CO/N_2	H_2O/N_2
PIS00	2.4	81.3	52.1	51.2	75.7	33.9	21.7	21.3	31.5
PIS03	2.0	79.6	48.4	50.7	67.5	39.8	24.7	25.4	33.8
PIS07	1.7	77.2	45.6	50.5	63.3	45.4	26.8	29.7	37.2
PIS15	1.4	75.8	42.3	50.3	57.5	54.1	30.2	35.9	40.1

[a] Permeability coefficients: 10^{-8} mol/(m^2 s Pa).

the hybrid membrane for H_2/N_2, CO_2/N_2, CO/N_2 and H_2O/N_2 reached 54.1, 30.2, 35.9 and 40.1, respectively.

V. ACKNOWLEDGMENT

This work was supported by the National Key Basic Research project of China (No.2001CCA03600).

[1] P. Mustoa, G. Ragosta, G. Scarinzi and L. Mascia, Polymer **45**, 4265 (2004).
[2] B. P. Lin, J. N. Tang, H. J. Liu, Y. M. Sun and C. W. Yuan, J. Solid State Chem. **178**, 650 (2005).
[3] G. M. Odegard, T. C. Clancy and T. S. Gates, Polymer **46**, 553 (2005).
[4] A. Kuntman and H. Kuntman, Microelectronics J. **31**, 629 (2000).
[5] C. C. Chang and W. C. Chen, Chem. Mater. **14**, 4242 (2002).
[6] G. Stefanini, Nucl. Instr. Meth. A **530**, 77 (2004).
[7] C. F. Li and S. H. Zhong, Catal. Today **82**, 83 (2003).
[8] S. Yano and K. Iwata, Mater. Sci. Eng. **C6**, 75 (1998).
[9] C. Xenopoulos, L. Mascia and S. J. Shaw, Mater. Sci. Eng. **C6**, 99 (1998).
[10] S. H. Zhong, C. F. Li and X. F. Xiao, J. Membr. Sci. **199**, 53 (2002).
[11] C. F. Li and S. H. Zhong, Acta Polym. Sin. **3**, 326 (2002).
[12] J. B. Guo and S. H. Zhong, Chin. J. Catal. **25**, 793 (2004).
[13] S. Monredon, A. Cellot, F. Ribot, C. Sanchez, L. Armelao, L. Gueneau and L. Delattre, J. Mater. Chem. **12**, 2396 (2002).
[14] Y. C. Chen and Y. G. Zhang, Chin. J. Chem. Phys. **19**, 1015 (2005).
[15] S. Loridant, J. Phys. Chem. B **106**, 13273 (2002).
[26] H. Lu, L. X. Wang, L. M. He, Y. L. Ten and X. R. Pan, J. Chem. Phys. **14**, 470 (2001).
[27] J. R. Zhang and L. Gao, J. Solid State Chem. **177**, 1425 (2004).
[18] M. Nandi, J. A. Conklin and J. L. Salvati, A. Sen, Chem. Mater. **3**, 201 (1991).
[19] T. M. Racheva and G. W. Critchlow, Thin Solid Films **292**, 299 (1997).
[20] C. F. Li and S. H. Zhong, J. Membr. Sci. **204**, 89 (2002).
[21] C. F. Li and S. H. Zhong, J. Chin. Cera. Soc. **2**, 19 (2002).
[22] C. T. Yen, W. C. Chen, D. J. Liaw and H. Y. Lu, Polymer **44**, 7079 (2003).
[23] R. A. Huang, L. S. Hou, Q. T. Zhao and S. H. Ren, Chin. J. Proc. Eng. **5**, 152 (2005).
[24] P. C. Chiang and W. T. Whang, Polymer, **44**, 2249 (2003).
[25] L. Liu, Q. H. Lu, J. Yin, X. F. Qian, W. K. Wang, Z. K. Zhu and Z. G. Wang, Mater. Chem. Phys. **74**, 210 (2002).
[26] Q. Hu and E. Marand, Polymer **40**, 4833 (1999).
[27] J. Zhang, B. J. Wang, X. Ju, T. Liu and T. D. Hu, Polymer **42**, 3697 (2001).

ISSN 1003-7713/DOI:10.1360/cjcp2007.20(2).197.6